Transitions in the kinetics and steady states of irreversible $A+BC$ surface-reaction models

B. Meng and W. H. Weinberg
Department of Chemical and Nuclear Engineering, University of California, Santa Barbara, Santa Barbara, California 93106

J. W. Evans
Ames Laboratory and Department of Mathematics, Iowa State University, Ames, Iowa 50011
(Received 8 January 1993)

The three-component irreversible surface-reaction model $A+BC\rightarrow AC+\frac{1}{2}B_2$ with infinite reaction rates between nearest-neighbor adspecies is studied by Monte Carlo simulations. For a square lattice the system evolves to a degenerate poisoned state exponentially in time, except for a narrow range of pressures in which a reactive quasi-steady-state exists. The latter poisons very slowly in time. For a hexagonal lattice a true reactive steady state occurs for a range of pressures bordered by continuous and discontinuous transitions to poisoned states. The latter behavior is observed by adding the reaction channel $A+B\rightarrow AB$ on a square lattice. Some properties of these models are elucidated by analysis of appropriate exact master equations and corresponding pair approximations. Other issues addressed include "extent of variability" of the degenerate poisoned states, the effect of finite reaction rates, and spatial correlations.

PACS number(s): 68.10.Jy, 05.70.Ln, 05.70.Fh, 05.40.+j

I. INTRODUCTION

The study of kinetic or nonequilibrium phase transitions has attracted much attention in both the physics and chemistry communities [1,2]. Surface reactions under flow conditions constitute a nonequilibrium system and can show complicated behavior, such as kinetic phase transitions [3]. Since spatial correlations are introduced under nonequilibrium conditions (even in the absence of interactions), traditional mean-field theory is technically inappropriate. Since lattice-gas modeling of the surface reactions has the capability to describe the influence of fluctuations, correlations, and interactions, many simplified surface-reaction models have been studied by Monte Carlo simulations for conditions far from equilibrium [4–9].

In this work, we focus on the properties of a lattice-gas model of the following Langmuir-Hinshelwood reaction scheme:

$$\begin{aligned} &A(\mathrm{g})+S\rightarrow A(\mathrm{a}) ,\\ &BC(\mathrm{g})+2S\rightarrow B(\mathrm{a})+C(\mathrm{a}) ,\\ &A(\mathrm{a})+C(\mathrm{a})\rightarrow AC(\mathrm{g})+2S , \end{aligned} \tag{1}$$

and

$$B(\mathrm{a})+B(\mathrm{a})\rightarrow B_2(\mathrm{g})+2S . \tag{2}$$

Here (g) denotes the gas-phase species, (a) denotes the absorbed species, and a vacant site on the surface is denoted by S. The impingement rate for A(g) is denoted by P_A and that for BC(g) by P_{BC}. These are normalized so that $P_A+P_{BC}=1$. Reactions between neighboring A(a) and C(a) and between neighboring B(a)'s occur instantaneously (i.e., with infinite reaction rate). This model, referred to as model 1 [10], is selected to mimic the known steps of the CO+NO reaction on certain transition metal surfaces [11] with A representing molecular carbon monoxide, B representing atomic nitrogen, and C representing atomic oxygen. We have, however, replaced the NO (or BC) adsorption and dissociation steps $BC(\mathrm{g})+S\rightarrow BC(\mathrm{a})$ and $BC(\mathrm{a})+S\rightarrow B(\mathrm{a})+C(\mathrm{a})$ by a single step. The catalytic surface is represented by a square lattice of adsorption sites (unless otherwise stated).

Monte Carlo simulations of this model have been conducted on $L\times L$ square lattices with periodic boundary conditions, where $L=40$, 80, and 120 lattice constants, and on a 40×40 hexagonal lattice. Time in these simulations is identified as the number of Monte Carlo steps (MCS), where each MCS is defined as one trial (adsorption attempt) per site. This is consistent with the specification in model 1 of the total impingement rate as unity. A trial proceeds by choosing A(g) with probability P_A or by choosing BC(g) with probability $1-P_A$. If the chosen species in A(g), a site on the lattice is chosen randomly; A(g) adsorbs on the lattice site and forms A(a) if the chosen site is empty (S). Then all nearest-neighbor (NN) sites are examined. If either one C(a) or more than one C(a) is found, the A(a) reacts immediately, either with the C(a) or with a randomly chosen C(a), and desorbs as AC(g), leaving both sites empty. If the originally chosen species is BC(g), two NN sites are randomly chosen on the lattice. The trial is a failure if either site is occupied; otherwise, the BC(g) dissociates and adsorbs on the two empty sites, forming B(a) and C(a). Then, all NN sites of C(a) and B(a) are examined. If one or more than one A(a) [B(a)] is found to be a NN of C(a) [B(a)], the C(a) [B(a)] reacts with a randomly chosen NN A(a) [B(a)] and desorbs as AC(g) [B_2(g)], leaving two vacant sites.

Our goals are to investigate the kinetics of this model, to locate and characterize any poisoning transitions that occur with varying P_A, and to quantify steady-state reac-

tivity. For a square lattice we observe a transition in the kinetics: an evolution to degenerate poisoned states occurs exponentially in time except for a narrow window P_A where a quasi-steady-state exists and poisoning occurs very slowly. For a hexagonal lattice conventional behavior, reported previously [7,8], is observed: a true reactive steady state is attained for a range of P_A bordered by continuous and discontinuous transitions to poisoned states. The presence of infinitely degenerate poisoned states violates the condition required by the conjecture of Grinstein, Lai, and Browne [12] for the continuous transition to be in the Reggeon field theory (RFT) universality class. This might allow a different universality class for the $A+BC$ model, just as was observed previously for the dimer-trimer model [9].

In Sec. II, we present our simulation results for the kinetics and poisoning transitions in this model. Some important exact results following from the hierarchical form of the master equations are described in Sec. III. These results are exploited in Sec. IV where we present the results of a mean-field theory at the level of the pair approximation which elucidates the simulation results. Various model modifications [finite reaction rates and the $A(a)+B(a)$ reaction] and spatial correlations are discussed in Sec. V. Some concluding remarks are provided in Sec. VI.

II. SIMULATION RESULTS

A. $A+BC$ reaction on a square lattice

We observed exponential decay of the AC-production rate per trial, i.e., $R_{AC}\sim e^{-kt}$, for $P_A \lesssim 0.213$ and $P_A \gtrsim 0.244$. The decay rate k is plotted as a function of P_A in Fig 1. The inset shows R_{AC} as a function of time for selected P_A (and starting from an initially empty lattice). In the narrow "reactive window" $0.213 \lesssim P_A \lesssim 0.244$, a reactive steady state seems to persist for several thousand MCS. However, a recent analysis by Brosilow and Ziff (BZ) [8], discussed below, indicates that no true reactive steady state can exist. This implies that in fact a "quasi-steady-state" was observed which must slowly poison. Assuming $R_{AC}\sim t^{-w}$ or $\ln t^{-\sigma}$ in this window, we find that $w\sim 0.1$ and $\sigma\sim 1.0$ in the interior of the window, increasing toward the edges. In this latter analysis, the location of the edges of the window is not well defined. More detailed studies in the center of the window, at $P_A=0.230$, yields $w=0.08\pm 0.02$ and $\sigma=0.69\pm 0.02$.

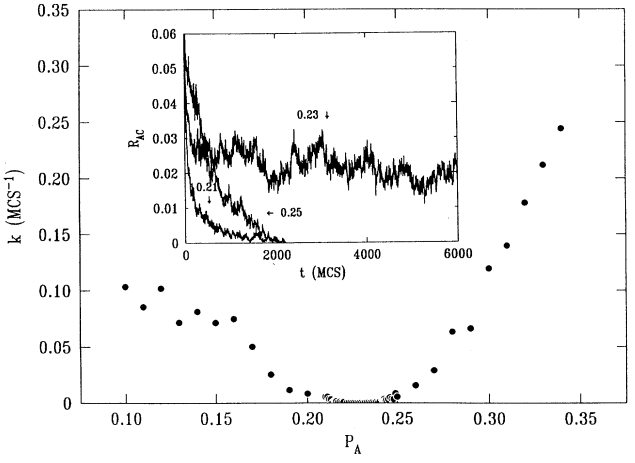

FIG. 1. Simulation results for the decay rate k as a function of P_A on an 80×80 square lattice. Inset is the production rates of AC per trial R_{AC} as a function of time (MCS) for selected values of P_A. These results are generated by Monte Carlo simulations on an 80×80 square lattice up to 6000 MCS.

To elucidate this behavior, consider an $L\times L$ lattice with L even. Following BZ, let $N_B^{\pm}$ denote the number of B's on the two checkerboard $c(2\times 2)$ sublattices constituting the full lattice. Define the $c(2\times 2)$ order parameter $M=N_B^{+}-N_B^{-}$, just as for an equilibrium lattice gas with NN repulsion. Then one has $-L^2/2\le M\le +L^2/2$ with the limits corresponding to poisoned states with perfect $c(2\times 2)$-B order and any distribution of A's and C's on the other sublattice. The key observation of BZ is that M undergoes a simple random walk (RW), a step of ± 1 occurring at each BC adsorption event. Thus poisoning occurs in no more than $O(L^4)$ steps at one of the $c(2\times 2)$-B ordered poisoned states or, more likely, at a disordered poisoned state *(vide infra)*. We note that the relationship between time t in MCS and the number of RW steps s is nonlinear: $\delta t\sim \delta s/L^2$ for short times, but $\delta t\sim \delta s$ near poisoning. However, we can assert that the mean poisoning time $t(L)$ is no greater than $O(L^4)$ MCS. According to ben-Avraham *et al.* [13], if a true reactive steady state exists, then $t(L)$ increases exponentially rather than as a power law of L. Thus, we conclude that no true steady state exists for this system. [Let $\sigma\equiv 2M/L^2$ define the normalized order parameter. Clearly, in the limit $L\to\infty$, $\langle\sigma^2\rangle$ and, of course, $\langle\sigma\rangle$ are zero for all finite times.]

This type of finite-size analysis was first applied to the simpler $A+B$ reaction model which poisons exponentially, except for $P_A=\frac{1}{2}$. It is interesting to note that when $P_A=\frac{1}{2}$, the slow decay of the reaction rate has the form t^{-w} or $\ln t^{-\sigma}$, with $w\approx 0.06$–0.08 and $\sigma\approx 0.5$ for $t\le O(10^4)$ [4,14–16] characteristic of the Voter model [16]. This decay in reaction rate is associated with a slow "reactive coarsening" of domains of A and B, reaction only occurring at the perimeter sites. This suggests that for the $A+BC$ model, at least at $P_A\approx 0.23$, the process proceeds by an analogous, slow reactive coarsening of $c(2\times 2)$-B domains.

Figure 2 shows several typical poisoned and quasi-steady-state configurations (for 6000 MCS) generated from simulations with an initially empty lattice. For small $P_A<0.213$, the poisoned state is mainly C covered with a substantial population of B's corralling a few mainly isolated A's. For high $P_A>0.244$, the roles of A and C are reversed. In the reactive window, one observes strong $c(2\times 2)$-B ordering, as suggested by the above arguments. Figure 3 shows the fractional coverage θ_J of J ($J=A,B,C$) as a function of P_A for poisoned states and quasi-steady-states at 6000 MCS.

Although there is no true, reactive steady state, the

behavior in the reactive window $0.213 \lesssim P_A \lesssim 0.243$ effectively mimics such a state. The insets in Fig. 3 show in detail the behavior of the quasi-steady-state θ_J (at 6000 MCS) across this window. Quasi-steady-state production rates for AC (R_{AC}) and θ_S are plotted as functions of P_A in Fig. 4. These rates vary approximately linearly with θ_S and satisfy $R_{AC}=2R_{B_2}$. Such relationships are characteristic of true steady states, as we shall demonstrate in Sec. III.

B. $A+BC$ reaction on a hexagonal lattice

Figure 5 shows several poisoned and steady-state configurations at 8000 MCS produced by the simulations

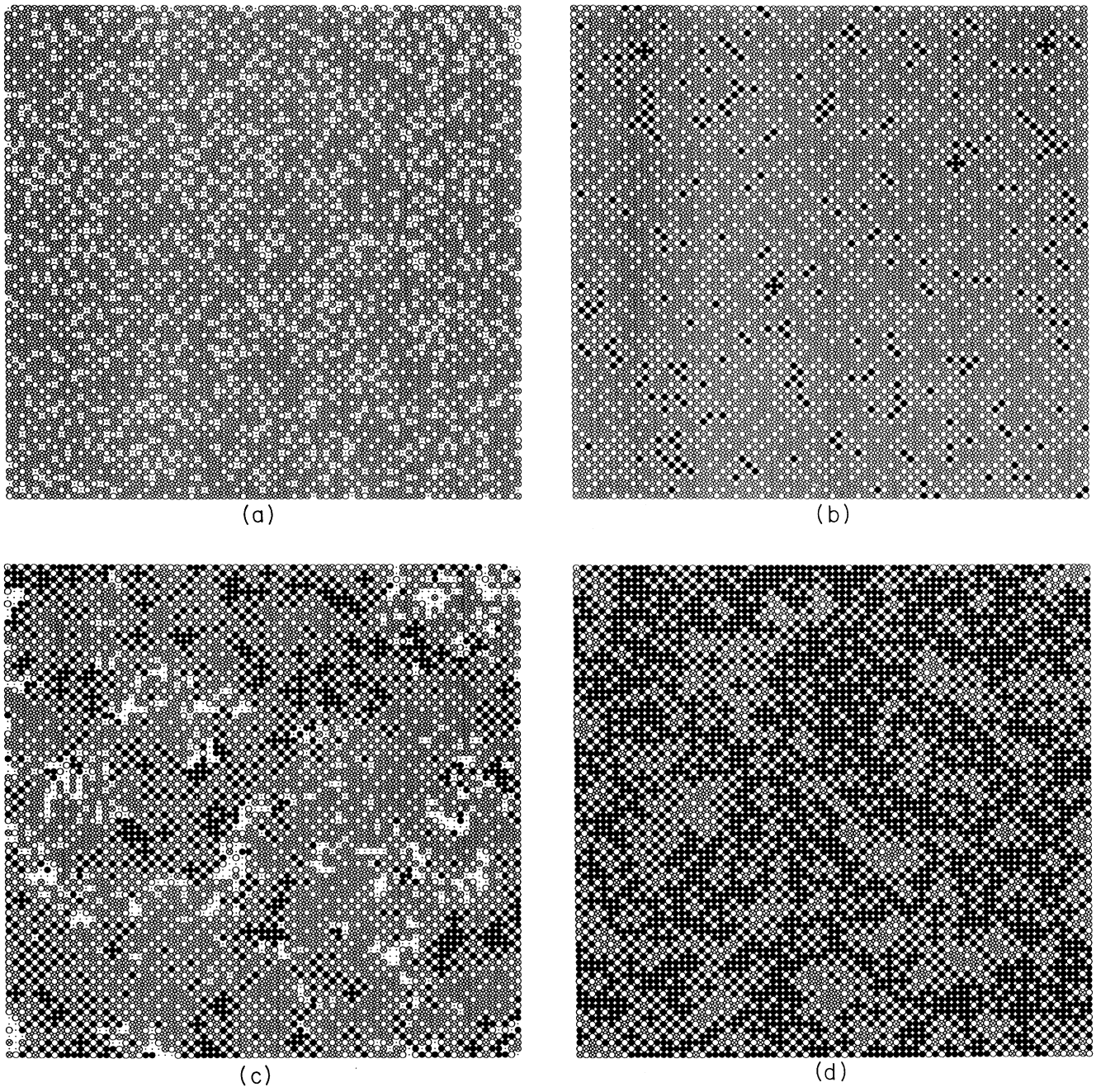

FIG. 2. (a)–(f) Typical configurations obtained from simulations in which P_A ranges from 0 to 0.25. The square lattice size is 80×80 for all these configurations, and the simulations start from an initially empty lattice. The dark circle represents A, the empty circle represent B, the cross circle represents C, and the smaller black dot represents the active lattice site on the surface. These snapshots are taken at 6000 MCS when (a) $P_A=0$, (b) $P_A=0.200$, (c) $P_A=0.230$, and (d) $P_A=0.250$.

on a 40×40 initially empty hexagonal lattice. Figure 6 shows the fractional coverage of each component, plotted as a function of P_A. When $0<P_A<P_1=0.172\pm0.001$, the surface becomes completely covered with isolated B's in a C-covered background. Here θ_A is identically zero since, unlike the square lattice, A's cannot be separated from C's by a wall of non-NN B's. When P_A is larger than $P_2=0.353\pm0.001$, the lattice becomes completely poisoned with isolated B's in an A-covered background. For $P_1<P_A<P_2$, the system achieves a reactive steady state. The transition at P_1 is continuous, and that at P_2 is discontinuous, just as in the monomer-dimer reaction model. Our estimate of P_2 agrees with the recent estimate of BZ [8], contrasting that of Yaldram and Khan [7]. We observe a propensity to form nuclei of the A-poisoned phase just below the discontinuous transition point. As on the square lattice in the reactive window, it appears that $R_{AC}=2R_{B_2}$. This behavior will be explained in Sec. III.

For nonequilibrium models which exhibit a continuous transition to a unique absorbing state, a conjecture of Grinstein, Lai, and Browne [12] states that they belong to the same "RFT" universality class. Examples of such models include the contact process [17], Schlögl's first model [18], directed percolation [19], Reggeon field theory [20], and the monomer-dimer reaction [3]. In contrast, models exhibiting a transition between an active state and an infinite degeneracy of poisoned states might belong to a different universality class or classes. Analysis of the dimer-trimer model and the $A+BC$ model on a hexagonal lattice could elucidate this issue. An

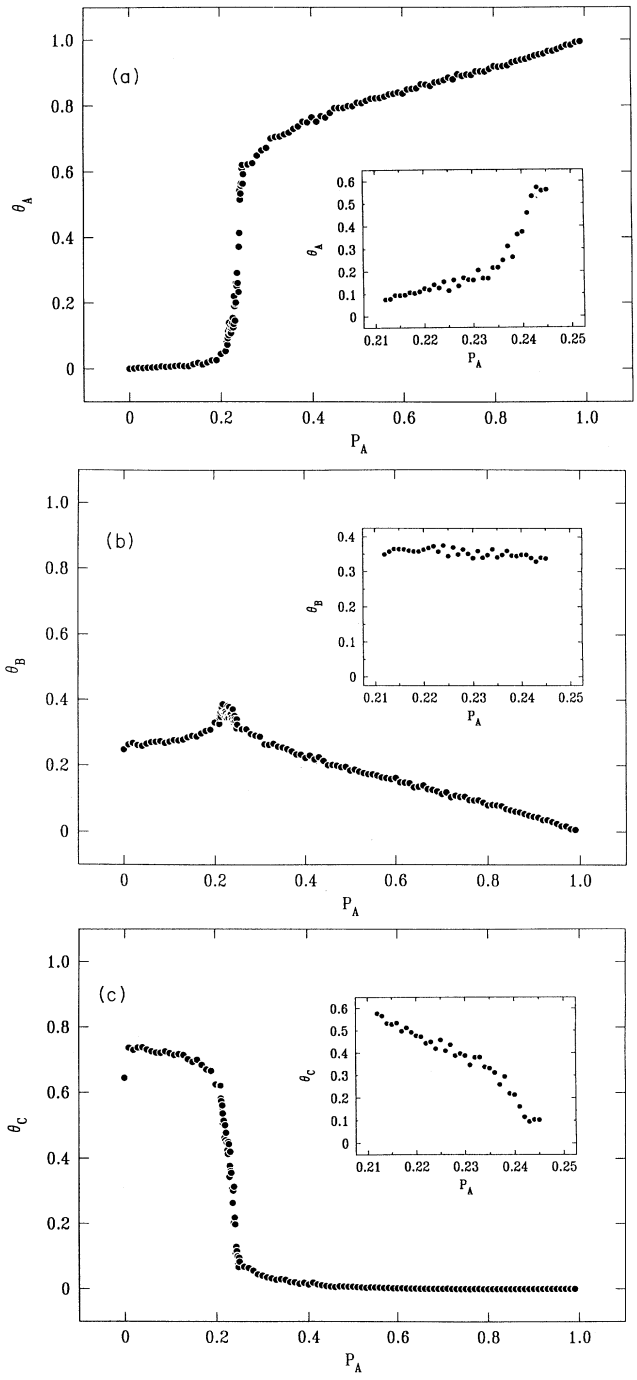

FIG. 3. Fractional coverages of A, B, and C as a function of P_A. These results are generated by Monte Carlo simulations on an 80×80 square lattice after 6000 MCS. Insets for $0.210<P_A<0.245$ are generated by Monte Carlo simulations on a 120×120 square lattice after 6000 MCS.

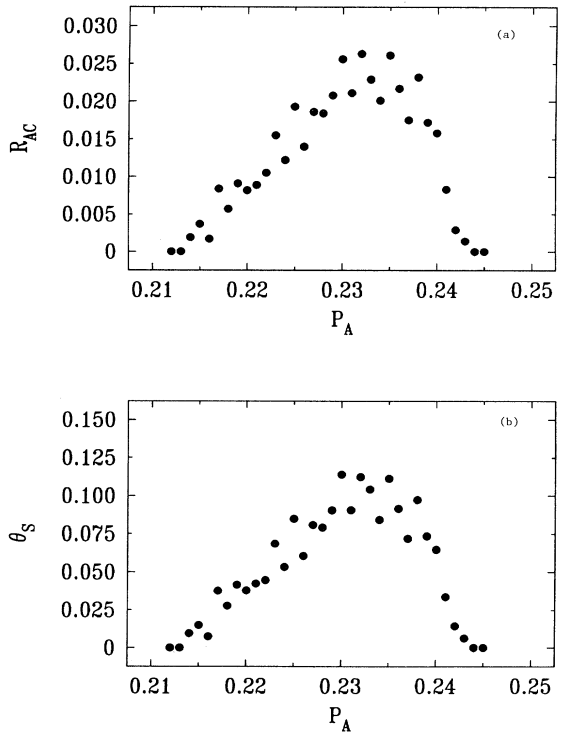

FIG. 4. (a) Steady-state reaction rates of AC as a function of P_A. These results are generated by Monte Carlo simulations on a 120×120 square lattice after 6000 MCS. (b) Fractional coverage of S as a function of P_A. These results are generated by Monte Carlo simulations on a 120×120 square lattice after 6000 MCS.

efficient and reliable technique for determination of critical exponents, and thus universality classes, is the so-called "epidemic analysis" [21–23]. One analyzes the survival probability and growth characteristics of an empty patch embedded in a poisoned background which is chosen as the unique poisoned state at the transition (*vide infra*). One could sample (inequivalent) selections of the position of the initial empty patch. However, a single choice should produce the same exponents due to self-averaging of the epidemic during the growth.

For any model with degenerate poisoned states, it is instructive to consider selecting initial conditions from some fixed nonpoisoned subset of phase space, e.g., lattices randomly filled with fractional coverages 0.0, 0.2, 0.4, 0.6, and 0.8 of C. For P_A in the reactive window, a unique reactive steady state is always achieved. However, outside this range, the system will evolve to a poisoned state which depends on the initial conditions. Here we provide the first discussion of the extent of this dependence.

The propensity for the system to "forget" its initial conditions is enhanced with increasing fluctuation amplitude and characteristic time τ for poisoning. Near a continuous poisoning transition at $P_A = P_1$, the correlation length ξ, measuring the fluctuation amplitude, diverges like $\xi \sim |P_A - P_1|^{-\nu}$, and τ diverges like ξ^{σ}. Here ν and σ are appropriate critical exponents [24]. Consequently, poisoned states obtained from various initial conditions should converge as $P_A \to P_1$. Our simulations are consistent with this behavior for initial fractional coverages of C, θ_C^0, which are 0.2, 0.4, 0.6, 0.8, and 0.95 (cf. Fig. 7). Of course, the dependence of the poisoned state on the initial conditions is *not* lost near a first-order transition where the correlation length remains finite. As an aside, we also note that this dependence is *not* lost for the model on a square lattice at the edges of the quasi-steady-state region, consistent with the absence of continuous transitions.

C. Reactive random dimer-filling problem

At $P_A = 0$, where only BC adsorbs on the lattice, the process is still nontrivial. For a square lattice, the surface finally reaches a jammed state with $\theta_C \cong 0.65$, $\theta_B \cong 0.24$,

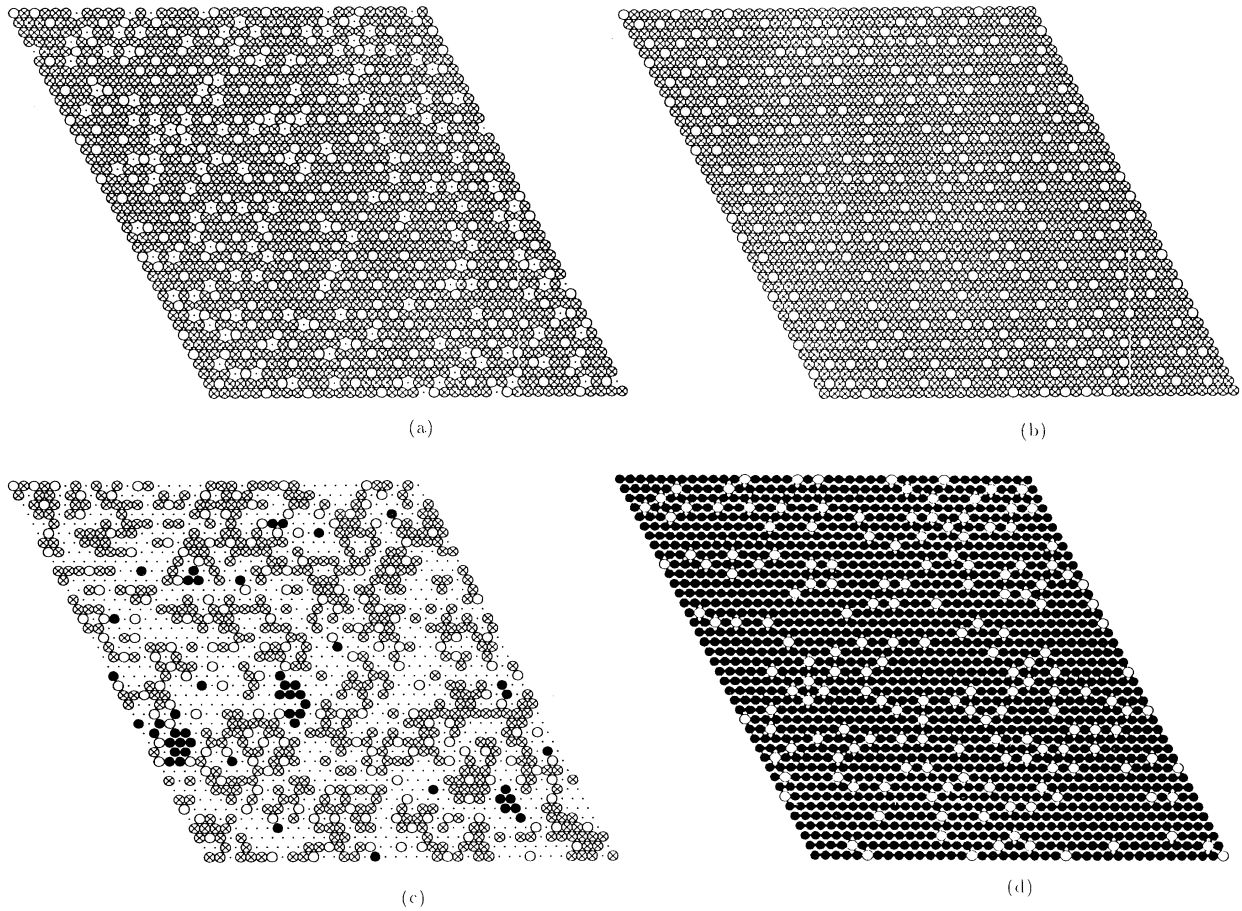

FIG. 5. (a)–(f) Typical configurations obtained from simulations in which P_A ranges from 0 to 0.355. The hexagonal lattice size is 40×40 for all these configurations. These snapshots are taken at 8000 MCS when (a) $P_A = 0$, (b) $P_A = 0.100$, (c) $P_A = 0.352$, and (d) $P_A = 0.355$. See caption to Fig. 2 for notation.

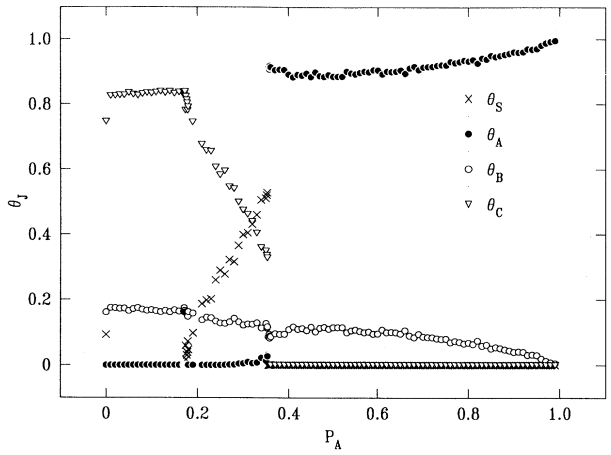

FIG. 6. Fractional coverage of S, A, B, and C as a function of P_A. These results are generated by Monte Carlo simulations on a 40×40 hexagonal lattice after 8000 MCS.

and $\theta_S \cong 0.11$, i.e., a total surface coverage of 0.89. As may be seen from Fig. 2(a), the jammed surface is covered with C, with isolated B's and S's. This should be compared with the conventional (irreversible) random dimer-filling problem [25], in which the jamming coverage is 0.9068 for a square lattice. For the hexagonal surface, we find that the jammed state occurs for $\theta_C \cong 0.76$, $\theta_B \cong 0.15$, and $\theta_S \cong 0.09$, a total surface coverage of 0.91 [cf. Fig. 5(a)], which is also different from the jamming coverage of 0.915 for conventional random dimer filling.

III. EXACT RESULTS FROM THE HIERARCHICAL RATE EQUATIONS

Obtaining exact rate equations in term of the coverages of the various surface species is somewhat complicated by

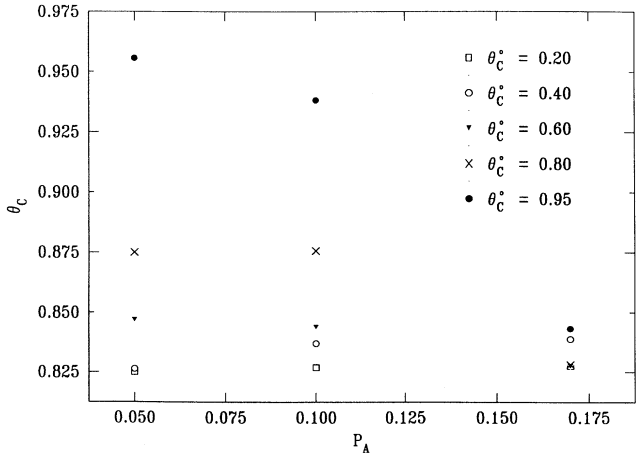

FIG. 7. Variation of the fractional coverage of C with different initial conditions θ_C^0 (fractional coverages of 0.2, 0.4, 0.6, 0.8, and 0.95 of randomly populated C) near the second-order phase transition point on a hexagonal 40×40 lattice for model 1.

the infinite reaction rates [26,27]. We sometimes denote probabilities of configurations by the configurations in square brackets taking care not to ignore correlations, i.e., $\theta_{SS} \neq \theta_S^2$ or $[SS] \neq [S]^2$, etc. Let A', B', and C' denote sites not filled with A, B, and C, respectively. It is also useful to introduce the following intermediate quantities (after normalizing the rates of adsorption correctly).

The total adsorption rates for A, B, and C are given by

$$T(A) = P_A \theta_S \ , \tag{3a}$$

$$T(B) = T(C) = (1 - P_A)\theta_{SS} \ . \tag{3b}$$

The nonreactive adsorption rates for A, B, and C are given by

$$N(A) = P_A \begin{bmatrix} & C' & \\ C' & S & C' \\ & C' & \end{bmatrix} , \tag{4a}$$

$$N(B) = (1 - P_A) \begin{bmatrix} & B' & \\ B' & S & S \\ & B' & \end{bmatrix} , \tag{4b}$$

$$N(C) = (1 - P_A) \begin{bmatrix} & A' & \\ A' & S & S \\ & A' & \end{bmatrix} , \tag{4c}$$

for a square lattice. For a hexagonal lattice, we obtain a similar form of these equations. The reactive adsorption rate of J ($J = A, B,$ and C) is given by

$$R(J) = T(J) - N(J) \ . \tag{5}$$

Hence the exact rate equations have the form (cf. Ref. [27])

$$\frac{d\theta_A}{dt} = N(A) - R(C) = N(A) + N(C) - T(C) \ , \tag{6a}$$

$$\frac{d\theta_C}{dt} = N(C) - R(A) = N(A) + N(C) - T(A) \ , \tag{6b}$$

$$\frac{d\theta_B}{dt} = N(B) - R(B) = 2N(B) - T(B) \ . \tag{6c}$$

We now consider steady-state properties obtained by setting all these rates to zero. Subtracting Eqs. (6a) and (6b) then implies that

$$\theta_{SS} = [P_A/(1 - P_A)]\theta_S \ . \tag{7}$$

Thus, at a continuous poisoning transition, θ_{SS} vanishes linearly with θ_S (rather than quadratically as in the classical mean-field theory). We will return to this point in Sec. IV. This identity holds even if we introduce surface diffusion into the model, since diffusion terms do not appear in the rate equations for species concentrations. However, diffusion would certainly modify the location of any transitions. One important consequence of Eq. (7) is that, since $\theta_{SS} \leq \theta_S$, any reactive steady state, and thus all nontrivial poisoning transitions, must occur for $P_A/(1 - P_A) \leq 1$ or $P_A \leq \frac{1}{2}$. This is consistent with the above simulation results. Although the above arguments and properties strictly apply to true reactive steady

states, it is clear that they will also apply for quasi-steady-states, as our simulation study confirms.

In general, reaction rates R_{AC} and R_{B_2} are given exactly by $R_{AC}=R(A)+R(C)=T(A)+T(C)-N(A)-N(C)$ and $R_{B_2}=R(B)=T(B)-N(B)$. Under steady-state conditions, it follows from Eq. (6) that $R_{AC}=T(A)=T(C)=P_A\theta_S$ and $R_{B_2}=T(B)/2=P_A\theta_S/2$. This explains the observed and obvious steady-state (and quasi-steady-state) relationship $R_{AC}=2R_{B_2}$. For the square lattice, this also illustrates that the quasi-steady-state reaction rates are approximately proportional to θ_S over a narrow reactive window in which $P_A/(1-P_A)$ is approximately constant.

IV. MEAN-FIELD RATE EQUATION ANALYSIS

A. Formulation

Consider first an application of the simplest mean-field theory, the "site approximation" which ignores all spatial correlations to describe the reactive steady state of the $A+BC$ model on a hexagonal lattice. Just as for the $A+B_2$ model, this approximation fails to produce the lower continuous kinetic phase transition associated with higher impingement rates of the diatomic dissociating molecule. This approximation sets $\theta_{SS}=\theta_S^2$. Thus, when θ_S is small, as required near a continuous transition, $\theta_{SS}\ll 1$, i.e., the requirement of two adjacent empty sites for dissociative adsorption of the diatomic becomes prohibitive (relative to single site adsorption). This precludes the possibility of such a nontrivial poisoning transition. However, in the lattice-gas reaction model, each reaction automatically creates an adjacent empty pair of sites, and this maintains their concentration at a level comparable to that of single empty sites. Indeed, this is demonstrated explicitly by Eq. (7), which shows that θ_{SS} vanishes linearly rather than quadratically with θ_S.

Since the site approximation is inadequate to describe the reactive steady state (or quasi-steady-state), one might contemplate utilizing higher-order (pair, triplet, etc.) "dynamic cluster approximations" [26,27]. However, even in the pair approximation, the associated rate equations for pair probabilities are so complicated as to provide little insight into the behavior of the reacting system. Thus we adopt here an alternative strategy which allows us to incorporate the essential pair correlations of empty sites, but to retain the level of simplicity of the site approximation. To this end, it is convenient to introduce conditional probabilities $q_S=\theta_{SS}/\theta_S$, $q_A=\theta_{AS}/\theta_S$, $q_{A'}=\theta_{A'S}/\theta_S$, etc., where q_S, q_A, and $q_{A'}$, for example, are the probabilities of finding a site which is empty, occupied by an A, and not occupied by an A, respectively, *given* an adjacent empty site. In the pair approximation, Eq. (6) can now be conveniently written in factorized form as

$$\frac{d\theta_A}{dt}=P_A\theta_S q_{C'}^z+(1-P_A)\theta_S q_S(q_{A'}^{z-1}-1)\ , \tag{8a}$$

$$\frac{d\theta_C}{dt}=P_A\theta_S q_{C'}^z+(1-P_A)\theta_S q_S q_{A'}^{z-1}-P_A\theta_S\ , \tag{8b}$$

$$\frac{d\theta_B}{dt}=(1-P_A)\theta_S q_S(2q_{B'}^{z-1}-1)\ , \tag{8c}$$

where z is the coordination number of the lattice of adsorption sites.

Let us now restrict our attention to the *reactive* steady state or (quasi-steady-state) where $d\theta_J/dt$ are zero (or very small). Equation (8c) implies that

$$q_B=1-q_{B'}=1-2^{-1/(z-1)}\ . \tag{9}$$

Thus q_B is equal to 0.2063 for a square lattice ($z=4$) and q_B is equal to 0.1294 for a hexagonal lattice ($z=6$). If we also exploit the exact identities $q_{C'}=q_B+q_S+q_A$ and $q_S=P_A/(1-P_A)$, Eq. (8a) reduces to

$$[1-2^{-1/(z-1)}+P_A/(1-P_A)+q_A]^z=1-(1-q_A)^{z-1}\ . \tag{10}$$

Solving Eq. (10) gives q_A as a function of P_A. A lower physical branch and an upper unphysical branch exist for $0\le P_A\le P_s$, and they merge at the "spinodal" point $P_A=P_s$. Within the context of the rate equations [Eqs. (8)], the lower branch corresponds to a stable "node," the upper branch corresponds to an unstable "saddle point," and P_s is a saddle-node bifurcation point [28]. One finds that $P_s=0.3020$ for $z=4$ and $P_s=0.3877$ for $z=6$.

Clearly, Eq. (10) does not prove the existence of continuous transitions or of a quasi-steady-state regime. However, it clearly suggests that if a discontinuous transition exists, then it should occur "slightly below" the spinodal point $P_A=P_s$. In such a transition q_A would jump from the lower branch of Eq. (10) to some poisoned state value. Exactly the same prediction is made by the site approximation [8], which can be obtained from Eq. (10) by simply replacing q_A with θ_A. Such a discontinuous transition, is, of course, realized for the hexagonal lattice, $z=6$ (cf. Fig. 6), but not for the square lattice.

A more detailed analysis is required to determine the location of the continuous transition or of the edges of the quasi-steady-state regime. It would suffice to determine the form of q_S as a function of θ_S. Since $q_S=P_A/(1-P_A)$, the inverse relationship $\theta_S=G(q_S)$ determines these locations via the roots of $0=G[P_A/(1-P_A)]$. Here we describe three basic forms for the q_S vs θ_S relationship: (i) the site-approximation form $q_S=\theta_S$; (ii) a quasilinear form $q_S=P_*/(1-P_*)+c\theta_S+\cdots$, where poisoning occurs at $P_A=P_*$ ($<P_s$); and (iii) a quasiparabolic form for $\theta_S=G(q_s)$ where $G[P_1/(1-P_1)]=G[P_2/(1-P_2)]=0$, poisoning occurring at $P_A=P_1$ and P_2, with $P_1<P_2$.

In an attempt to determine the q_S vs θ_S relationship, one naturally starts with an analysis of the rather complicated $d\theta_{SS}/dt$ equation at the level of the pair approximation. Here we can at least factor the configurational probabilities in terms of the previously introduced quantities θ_S, q_S, q_A, and q_B. In fact, one can extract the steady-state behavior of θ_S from that of these other quantities which was determined above. However, this analysis fails to produce behavior of θ_S consistent with nontrivial continuous transitions. Presumably, the pair

approximation, which does a reasonable job of describing the configurations appearing in Eq. (6), is less adequate to treat the more compact and highly connected configurations appearing in the θ_{SS} equation. Thus higher-order approximations would be required.

B. Comparison with simulations

For the square-lattice simulations ($z=4$), it is clear that case (iii) applies (*vide supra*). The locations of the edges of the quasi-steady-state regime were estimated to be $P_1=0.213$ and $P_2=0.244$, well below the value of $P_s=0.3020$, as expected. From simulations, we find that q_B is roughly constant across the reactive window $P_1 \le P_A \le P_2$ ($q_B \cong 0.244$ when $P_A=0.22$ and $q_B \cong 0.257$ when $P_A=0.23$) and has a value consistent with Eq. (9). The value of q_A increases across the reactive region, as predicted qualitatively by Eq. (10), but q_A is considerably smaller in magnitude than that which is predicted. The quasiparabolic form of $\theta_S=G(q_S)=G[P_A/(1-P_A)]$ is evident from Fig. 4(b).

For the hexagonal lattice simulations ($z=6$), it is clear that case (ii) applies. Here $P_1=0.172$ is well below P_s. The location of the discontinuous transition $P_A=0.353$ is "just below" the spinodal $P_s=0.3877$, as one would expect. The quasilinear form of θ_S vs q_S is evident in Fig. 6. From simulations, we find that q_B is roughly constant across the reactive window in this case also and has a value consistent with Eq. (9). In particular, we find $q_B \cong 0.14$ when $P_A=0.18$, $q_B \cong 0.12$ when $P_A=0.25$, and $q_B \cong 0.13$ when $P_A=0.35$. The value of q_A is also consistent with that predicted from Eq. (10).

V. EXTENSIONS

A. Finite reaction rates

It is instructive to comment on the generalization of the above reaction model to the case of finite reaction rates, i.e., $A(a)+C(a) \rightarrow AC(g)+2S$ with rate k_{AB} and $B(a)+B(a) \rightarrow B_2(g)+2S$ with rate k_{B_2}. Then the form of the exact rate equations is simplified, compared to the case of infinite reaction rates given by Eq. (6), to become

$$\frac{d\theta_A}{dt}=P_A\theta_S-zk_{AC}\theta_{AC}\ , \tag{11a}$$

$$\frac{d\theta_C}{dt}=(1-P_A)\theta_{SS}-zk_{AC}\theta_{AC}\ , \tag{11b}$$

$$\frac{d\theta_B}{dt}=(1-P_A)\theta_{SS}-zk_{B_2}\theta_{BB}\ , \tag{11c}$$

where again z denotes the lattice coordination number.

By comparison with $A+B_2$ reaction-model studies, we expect the behavior of the $A+BC$ model for finite and infinite reaction rates to be similar. Here we restrict our attention to properties of the steady state (or quasi-steady-state). Indeed, from Eq. (11), it follows immediately that the exact identity Eq. (7), i.e., $\theta_{SS}=[P_A/(1-P_A)]\theta_S$, is also satisfied for finite rates. Furthermore, again all nontrivial transitions or quasi-steady-states must occur for $P_A<\frac{1}{2}$. Application of the site approximation to Eq. (11) fails to produce nontrivial continuous poisoning transitions for the same reason as in the infinite reaction-rate case. Factorization of pair probabilities also leads to the incorrect prediction that poisoned states have $\theta_B=0$ and either θ_A or $\theta_C=0$. However, retaining θ_{SS}, θ_{BB}, and θ_{AC} pairs as variables and factorizing other configurations, or even implementing the full pair approximation, produces inadequate results.

The reaction-limited regime k_{AC} and $k_{B_2} \rightarrow 0$ is of special interest since some exact analysis is possible. Here the surface is always completely covered, i.e., $\theta_A+\theta_B+\theta_C=1$. As soon as a reaction occurs, the empty pair that is created is immediately filled by a BC or by two A's. (In the latter case, one site is first filled by an A leaving an isolated empty site which must necessarily be filled by a second A.) The probabilities of these two events are in the ratio of $(1-P_A)/2$ to $2P_A$. Here $(1-P_A)/2$ is the adsorption probability of BC at a specific empty pair (only half of the adsorption attempts at rate $1-P_A$ have the required orientation) and $2P_A$ is the total adsorption probability of A at the pair of empty sites. Since in this model the reactive A and C desorption rates are always equal, at steady state the adsorption rates must also be equal. Consequently, one has $(1-P_A)/2=2\times 2P_A$, and hence $P_A=\frac{1}{9}$. The extra factor of 2 reflects the fact the empty pair is filled with two A's, or one C and one B. Consequently, the only possibility for a reactive steady state in the reaction-limited regime is at $P_A=\frac{1}{9}$. Most likely, however, this choice of P_A also leads to poisoning, albeit slowly (*vide infra*).

An analogous situation to that described here is observed in the $A+B_2$ model for finite-reaction rate k [14]. Here the width of the reactive window vanishes as $k \rightarrow 0$, and $k=0^+$ corresponds to the Voter model for spatiotemporal dynamics of party support in a two-party state [29]. Here it is known that slow coarsening occurs at the "balance point" of equal A and B adsorption rates (i.e., there is only a trivial steady state).

B. Side reaction effect: Model2

We have demonstrated that, if we change the lattice geometry, we can change the intrinsic nature of the stochastic process. We expect that if we add another reaction channel to decrease the possibility of poisoning, we would also increase the reactivity of the system and modify the nature of the poisoning transition. We prove our expectation by the explicit study of a revised model, which we call model 2, in which we add an additional reaction channel

$$A(a)+B(a) \rightarrow AB(g)+2S \tag{12}$$

to the mechanism of model 1.

Simulations for infinite reaction rates on a square lattice show a continuous poisoning transition for "low" $P_A=0.262\pm0.001$ and a discontinuous transition to a trivial A-poisoned state for "high" $P_A=0.501\pm0.01$. Figure 8 shows typical configurations obtained from

simulations and Fig. 9 shows the fractional coverage of each component plotted as a function of P_A. It is clear that the poisoned state at low values of P_A is still degenerate, consisting of isolated B's in a C-covered background, whereas the poisoned state at high values of P_A consists of only a single component A. For $0.262\pm0.001 \leq P_A \leq 0.501\pm0.001$, the system eventually reaches a reactive steady state. We also observe a propensity to form nuclei of the A-poisoned phase just below the discontinuous transition point; cf. Fig. 9(d).

Reaction rates of AC, B_2, and AB as functions of P_A and θ_S are plotted in Figs. 10 and 11, respectively. As in the case of model 1, the reaction rate of each product shows approximately a linear relationship with the fractional coverage of bare sites. This behavior is explained as follows. Since the total reaction rates for B and C must be equal in the reactive steady state, one has $R_{AC}=R_{AB}+2R_{B_2}$. Let $T(J)$ denote the total adsorption rate for species J, as previously. Then from either intuitive reasoning or detailed mathematical analysis (cf. the Appendix), it is clear that

$$R_{AC}=T(C)=(1-P_A)\theta_{SS} \ , \tag{13a}$$

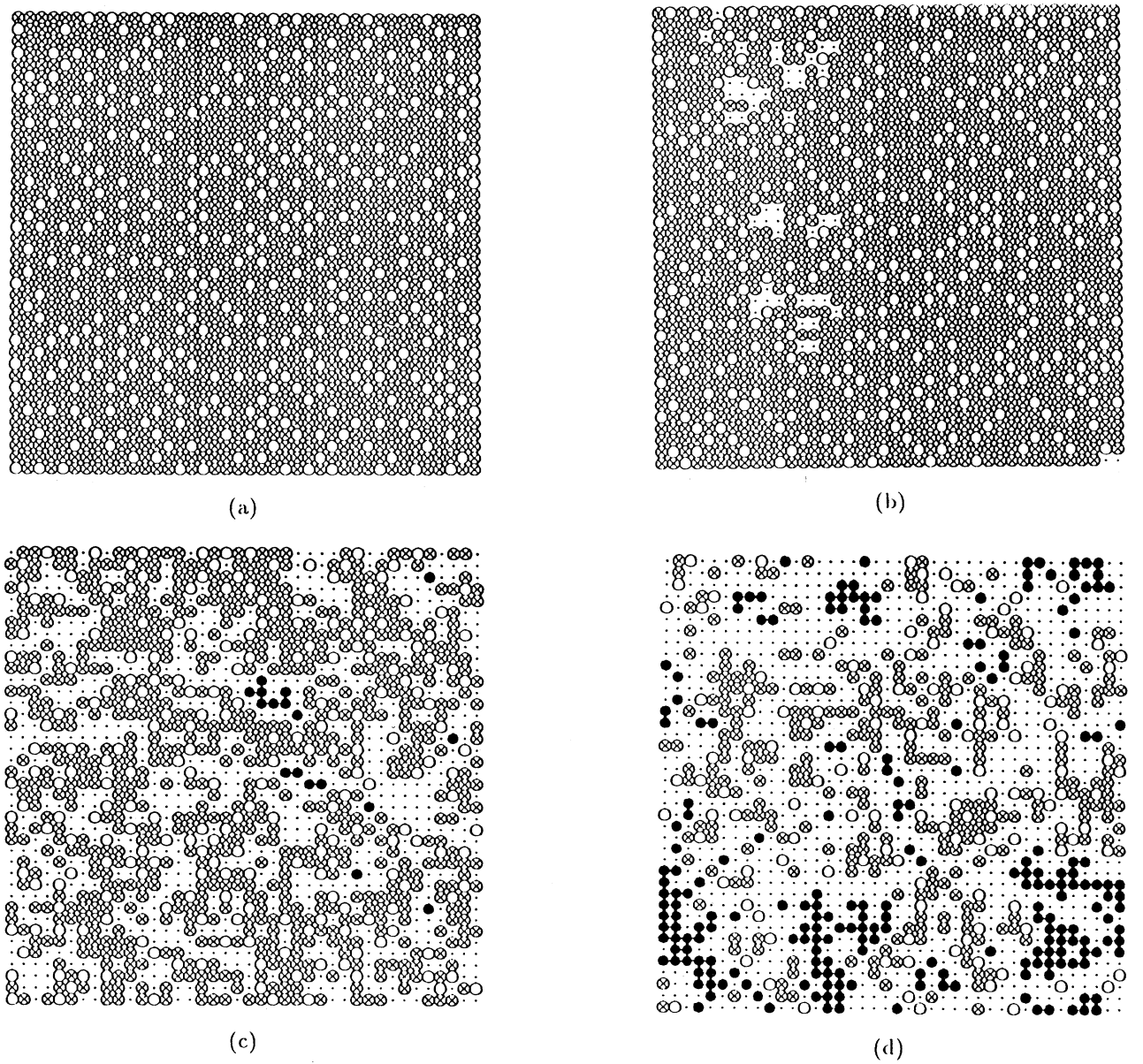

FIG. 8. (a)–(f) Typical configurations obtained from simulations for model 2 in which P_A ranges from 0.200 to 0.501. The square lattice size is 40×40 for all these configurations. These snapshots are taken at 6000 MCS when (a) $P_A=0.200$, (b) $P_A=0.262$, (c) $P_A=0.400$, and (d) $P_A=0.501$. See caption to Fig. 2 for notation.

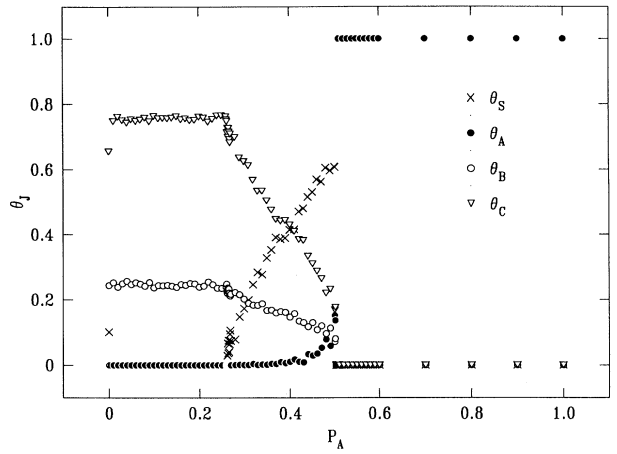

FIG. 9. Fractional coverages of S, A, B, and C as a function of P_A. These results are generated by Monte Carlo simulations on an 80×80 square lattice after 6000 MCS.

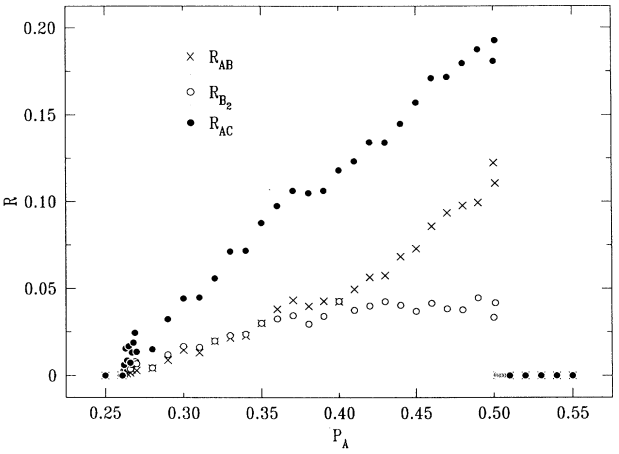

FIG. 10. Reaction rates of AB, B_2, and AC as a function of P_A. These results are generated by Monte Carlo simulations on a 40×40 square lattice after 6000 MCS.

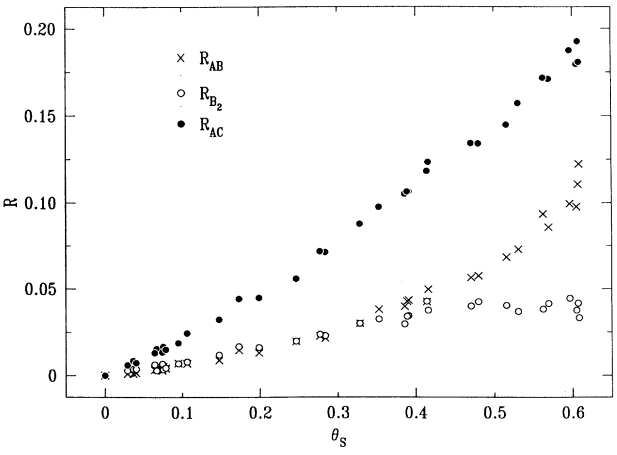

FIG. 11. Reaction rates of AB, B_2, and AC as a function of θ_S. See caption of Fig. 10 for details.

$$R_{AB}=T(A)-T(C)=P_A\theta_S-(1-P_A)\theta_{SS}\ . \tag{13b}$$

Consequently, one has

$$R_{B_2}=[T(B)-R_{AB}]/2=(1-P_A)\theta_{SS}-P_A\theta_S/2\ . \tag{14}$$

Since these reaction rates are non-negative, we conclude that reactive steady states require $P_A<\frac{2}{3}$ and

$$(1-P_A)\theta_{SS}\le P_A\theta_S\le 2(1-P_A)\theta_{SS}\ . \tag{15}$$

Thus, although θ_{SS} is to trivially related to θ_S as in model 1, there clearly exists a quasilinear relationship with, for example, θ_{SS} vanishing linearly with θ_S at the continuous transition. Consequently, we expect reaction rates to vary approximately linearly with θ_S.

C. Spatial correlations

For a detailed understanding of the poisoning transitions, one could also investigate many other questions concerning correlations and island sizes in the reactive and poisoned steady states of these models. Here we make the following brief observations concerning the behavior of the short-range order as measured by the NN correlation function $C(JJ)=\theta_{JJ}-\theta_J^2$ with $J=A$ or C.

(i) For all three models, the C's are anticlustered in the low P_A poisoned state. As P_A increases, the strength of the anticlustering decreases, but persists into the reactive window. At the upper end of the reactive window, the C's become weakly clustered.

(ii) For model 1 on a square lattice, the A's are weakly clustered throughout the quasireactive window, $P_1<P_A<P_2$, with a maximum $C(AA)$ of about 0.03. For model 1 on a hexagonal lattice and model 2 (both of which have an upper discontinuous transition), the A's are uncorrelated throughout most of the reactive window and only become weakly clustered near the discontinuous transition at P_2. Presumably this is a precursor to nucleation of the A-rich poisoned phase.

(iii) The A's are weakly anticlustered in the degenerate high P_A poisoned states of model 1.

VI. CONCLUSIONS

We have investigated, by Monte Carlo simulations and a mean-field analysis, a three-component irreversible surface reaction model $A+BC\rightarrow AC+\frac{1}{2}B_2$ with infinite reaction rates. For a square lattice, we find evolution to degenerate poisoned states exponentially in time, except for $P_1=0.213\pm0.001<P_A<P_2=0.244\pm0.001$ where a quasi-steady-state exists which poisons very slowly. If the substrate is changed to a hexagonal lattice, a reactive steady state is achieved in a region between a second-order kinetic phase transition at $P_1=0.172\pm0.001$ and a first-order kinetic phase transition at $P_2=0.353\pm0.001$. Incorporating another reaction channel $A+B\rightarrow AB$ on the square lattice, we also find a reactive steady state between a second-order transition at $P_1=0.262\pm0.001$ and a first-order transition at $P_2=0.501\pm0.001$. This behavior is reminiscent of the $A+B_2$ surface reaction model [3]. We support several of these observations by a

mean-field analysis at the level of the pair approximation. By utilizing conditional probabilities, together with an exact identity relating empty pair and site probabilities, we illustrate this basic behavior avoiding the complexity of the full pair equations. We also addressed the "extent of variability" of the degenerate poisoned states and the effect of finite reaction rates.

ACKNOWLEDGMENTS

W.H.W. and B.M. gratefully acknowledge the financial support of the National Science Foundation (Grant No. CHE-9300020). J.W.E. acknowledges valuable discussions with R. M. Ziff and B. Brosilow. He was supported for this work by the Division of Chemical Sciences (U.S. DOE) through Ames Laboratory. Ames Laboratory is operated by Iowa State University under Contract No. W-7405-ENG-82.

APPENDIX: EXACT HIERARCHICAL EQUATIONS FOR MODEL 2

Let Z denote A or B, Y denote C or B, and $Z'(Y')$ denote not $Z(Y)$. In developing exact rate equations (for a square lattice), it is convenient to introduce total adsorption rates $T(J)$ and nonreactive adsorption rates $N(J)$ for species $J=A$, B, and C. These have the form

$$T(A)=P_A\theta_S\ , \tag{A1a}$$

$$T(B)=T(C)=(1-P_A)\theta_{SS}\ , \tag{A1b}$$

as for model 1, and

$$N(A)=P_A\begin{bmatrix} & Y' & \\ Y' & S & Y' \\ & Y' & \end{bmatrix}\ , \tag{A2a}$$

$$N(B)=(1-P_A)\begin{bmatrix} & Z' & \\ Z' & S & S \\ & Z' & \end{bmatrix}\ , \tag{A2b}$$

$$N(C)=(1-P_A)\begin{bmatrix} & A' & \\ A' & S & S \\ & A' & \end{bmatrix}\ . \tag{A2c}$$

The total reactive desorption rates $R(J)=T(J)-N(J)$ are naturally decomposed as $R(J)=\sum_K R_K(J)$ where $R_K(J)$ is the component of $R(J)$ due to reaction of J with K. Specifically, one has

$$R(A)=R_B(A)+R_C(A)\ , \tag{A3a}$$

$$R(B)=R_A(B)+R_B(B)\ , \tag{A3b}$$

$$R(C)=R_A(C)=T(C)-N(C)\ . \tag{A3c}$$

The exact forms of the $R_K(J)$ are rather complicated and are thus not given here. The rate equations can be written as

$$\frac{d\theta_A}{dt}=N(A)-R_A(B)-R(C)\ , \tag{A4a}$$

$$\frac{d\theta_C}{dt}=N(C)-R_C(A)\ , \tag{A4b}$$

$$\frac{d\theta_B}{dt}=N(B)-R_B(B)-R_B(A)\ , \tag{A4c}$$

and the rates of the three reactions are given by

$$R_{AC}=R_C(A)+R(C)\ , \tag{A5a}$$

$$R_{B_2}=R_B(B)\ , \tag{A5b}$$

$$R_{AB}=R_B(A)+R_A(B)\ . \tag{A5c}$$

In the reactive steady state, one has the following simplifications: Eq. (A4b) implies that $R_C(A)=N(C)=T(C)-R(C)$, which implies from Eq. (A5a) that $R_{AC}=T(C)=(1-P_A)\theta_{SS}$; Eq. (A4a) implies that

$$\begin{aligned} R_A(B)&=N(A)-R(C)\\ &=T(A)-R(A)-R(C)\\ &=T(A)-T(C)-R_B(A) \end{aligned}$$

using the result for R_{AC}. Consequently, one finds $R_{AB}=T(A)-T(C)$. Finally, a more complicated calculation using Eq. (A4c) and the above results shows that $R_{B_2}=\frac{1}{2}[T(B)+T(C)-T(A)]$. These results confirm Eqs. (13) and (14) presented above.

[1] G. Nicolis and I. Prigogine, *Self-Organization in Nonequilibrium Systems* (Wiley Interscience, New York, 1977).
[2] H. Haken, *Synergetics* (Springer-Verlag, New York, 1977).
[3] R. M. Ziff, E. Gulari, and Y. Barshad, Phys. Rev. Lett. **56**, 2553 (1986).
[4] J. W. Evans, Langmuir **7**, 2514 (1991), and references therein.
[5] H. C. Kang, W. H. Weinberg, and M. W. Deem, J. Chem. Phys. **93**, 6841 (1991).
[6] M. W. Deem, W. H. Weinberg, and H. C. Kang, Surf. Sci. **276**, 99 (1992).
[7] K. Yaldram and M. A. Khan, J. Catal. **131**, 369 (1991).
[8] B. J. Brosilow and R. M. Ziff, J. Catal. **136**, 275 (1992).
[9] J. Köhler and D. ben-Avraham, J. Phys. A **24**, L621 (1991).
[10] B. Meng and W. H. Weinberg (unpublished).
[11] S. H. Oh, G. B. Fisher, J. E. Carpenter, and D. W. Goodman, J. Catal. **100**, 360 (1986); Th. Fink, J.-P. Dath, R. Imbihl, and G. Ertl, Surf. Sci. **245**, 96 (1991); Th. Fink, J.-P. Dath, R. Imbihl, and G. Ertl, J. Chem. Phys. **95**, 2109 (1991).
[12] G. Grinstein, Z. W. Lai, and D. A. Browne, Phys. Rev. A **40**, 4820 (1989).
[13] D. ben-Avraham, S. Redner, D. B. Considine, and P. Meakin, J. Phys. A **23**, L613 (1990); D. ben-Avraham, D. B. Considine, P. Meakin, S. Redner, and H. Takayasu, *ibid.* **23**, 4297 (1990).
[14] J. W. Evans and M. S. Miesch, Phys. Rev. Lett. **66**, 833 (1991).

[15] P. Meakin and D. Scalapino, J. Chem. Phys. **87**, 731 (1987).
[16] J. W. Evans and T. R. Ray, Phys. Rev. E **47**, 1018 (1993).
[17] T. Harris, Ann. Prob. **2**, 969 (1974).
[18] F. Schlögl, Z. Phys. B **253**, 147 (1972).
[19] J. Blease, J. Phys. C **10**, 917 (1977); **10**, 923 (1977); **10**, 3461 (1977).
[20] R. C. Brower, M. A. Furman, and M. Moshe, Phys. Lett. **76B**, 213 (1978).
[21] P. Grassberger and A. De La Torre, Ann. Phys. (N.Y.) **122**, 373 (1979).
[22] I. Jensen, H. C. Forgedby, and R. Dickman, Phys. Rev. A **41**, 3441 (1990).
[23] M. Dumont, P. Dufour, B. Sente, and R. Dagonnier, J. Catal. **122**, 95 (1990).
[24] T. Aukrust, D. A. Browne, and I. Webman, Phys. Rev. A **41**, 5294 (1990).
[25] R. S. Nord and J. W. Evans, J. Chem. Phys. **82**, 2795 (1985).
[26] R. Dickman, Phys. Rev. A **34**, 4246 (1986).
[27] J. W. Evans and M. S. Miesch, Surf. Sci. **245**, 401 (1991).
[28] J. Guckenheimer and P. Holmes, *Nonlinear Oscillations, Dynamical Systems and Bifurcations of Vector Fields,* edited by F. John, J. E. Marsden, and L. Sirovich, Applied Mathematical Sciences Vol. 42 (Springer-Verlag, New York, 1983).
[29] T. M. Liggett, *Interacting Particle Systems* (Springer-Verlag, New York, 1985).